ORGANOMETALLICS

pubs.acs.org/Organometallics Article

A Cationic Magnesium-Based Dithiolene Radical

Yuzhong Wang, Phuong M. Tran, Boris Dzikovski, Yaoming Xie, Pingrong Wei, April A. Rains, Hamid Asadi, Ramaraja P. Ramasamy, Henry F. Schaefer, III, and Gregory H. Robinson*

Cite This: *Organometallics* 2022, 41, 527−531 **Read Online**

ACCESS | Metrics & More | Article Recommendations | Supporting Information

ABSTRACT: Magnesium-based dithiolene radical adduct (**6**$^{\bullet}$), the first Group 2 element based dithiolene radical, was synthesized via $Ph_3C^+[B(C_6F_5)_4]^-$-mediated one-electron oxidation of the THF-solvated neutral magnesium dithiolene complex (**5**). Single-crystal X-ray diffraction analysis reveals that **6**$^{\bullet}$ exists as a magnesium-based dithiolene radical cation/$[B(C_6F_5)_4]^-$ anion pair. While electron paramagnetic resonance (EPR) and computations indicate the predominantly dithiolene ligand-based radical character of **6**$^{\bullet}$, the weak satellite feature of the EPR spectrum of **6**$^{\bullet}$ originates from an admixture of the ^{25}Mg isotope ($I = 5/2$) with a natural abundance of ca. 10%. The redox properties of **6**$^{\bullet}$ were explored using cyclic voltammetry.

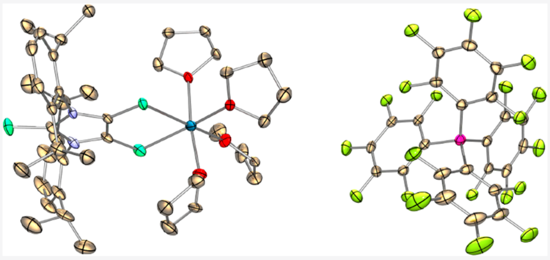

■ INTRODUCTION

The radical character of dithiolene ligands in transition metal complexes has attracted significant attention since it was first proposed by Gray nearly six decades ago.[1−14] Sulfur K-edge X-ray absorption spectroscopy (XAS) has provided compelling experimental support for the noninnocence of dithiolene ligands in corresponding transition metal complexes.[3] In contrast to the extensive development of these transition metal analogs, main group element-based dithiolene radicals are rare. Transition metal free dithiolene radical species have been mainly explored by computations and electron paramagnetic resonance techniques.[15−18]

This laboratory recently reported a lithium-based dithiolene radical (**1**$^{\bullet}$) (Figure 1),[19] synthesized by trisulfurization of the corresponding anionic *N*-heterocyclic dicarbene (Scheme 1). In addition to being the first structurally characterized main group element-based dithiolene radical, **1**$^{\bullet}$, also provided a convenient platform from which the promising chemistry of other main group element-based dithiolene radical species could be explored. To this end, two boron-based dithiolene radicals[20] (**2**$^{\bullet}$ and **3**$^{\bullet}$) and a metal-free "naked" dithiolene radical anion[21] (**4**$^{\bullet-}$) (with an imidazolium $[\{(Me)CN(i\text{-}Pr)\}_2CH]^+$ countercation) were recently reported by this laboratory (Figure 1). The "naked" dithiolene radical, **4**$^{\bullet}$, with NHSi^{Dipp} (Dipp = 2,6-diisopropylphenyl) and hexasulfide $[\{(Me)CN(i\text{-}Pr)\}_2CH]^+{}_2[S_6]^{2-}$, was shown to engage in

Scheme 1. Synthesis of 6$^{\bullet a}$

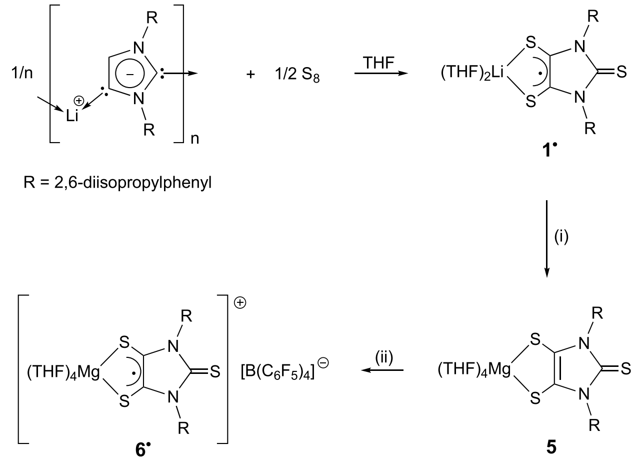

^{a}(i) MesMgBr, THF; (ii) $Ph_3C^+[B(C_6F_5)_4]^-$, toluene.

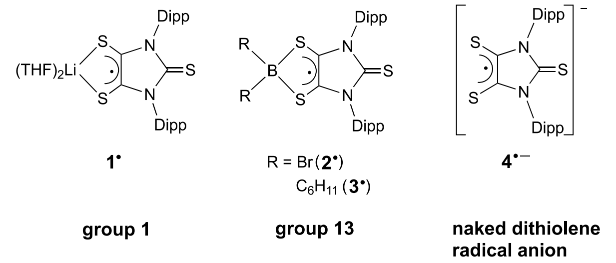

group 1 **group 13** **naked dithiolene radical anion**

Figure 1. Main group element based dithiolene radicals and naked dithiolene radical anion.

Received: October 22, 2021
Published: February 28, 2022

https://doi.org/10.1021/acs.organomet.1c00607

synergic THF ring-opening reactions.[21] Notably, the literature reveals a paucity of Group 2 element based dithiolene radicals. Herein, we report the synthesis,[22] UV/vis and EPR spectra,[22] cyclic voltammetry studies,[22] molecular structure,[22] and computations[22] of the first magnesium-based dithiolene radical adduct (**6**$^{\bullet}$).

■ RESULTS AND DISCUSSION

Reaction of **1**$^{\bullet}$ with mesitylmagnesium bromide afforded the $(THF)_4$-coordinated magnesium dithiolene complex (**5**).[23] Compound **5** could be readily converted to the corresponding THF-solvated five-coordinate magnesium bis(dithiolene) dianion via carbene-mediated partial hydrolysis.[23] Intrigued by its redox capabilities, we explored the room temperature reaction of **5** with $Ph_3C^+[B(C_6F_5)_4]^-$ (in a 1:1 molar ratio). This reaction resulted in one-electron oxidation of **5**, giving **6**$^{\bullet}$ as a cationic magnesium-based dithiolene radical (with $[B(C_6F_5)_4]^-$ as the counteranion). Radical **6**$^{\bullet}$ was isolated as dark purple-blue crystals via low-temperature recrystallization from a 1,2-difluorobenzene/hexane mixed solvent.[22] The UV−vis absorption spectrum of **6**$^{\bullet}$ (in toluene) reveals two strong broad absorptions at 580 and 622 nm (Figure S1).[22] By comparison, the broad absorptions for **1**$^{\bullet}$ are observed at 554 and 579 nm,[19] while those for the boron dithiolene radicals are observed at 606, 654 nm (**2**$^{\bullet}$) and 596, 630 nm (**3**$^{\bullet}$).[20] The TD-DFT method (CAM-B3LYP/6-311G**,[24] in toluene solvent) was utilized in studying the UV−vis spectrum of $[\mathbf{6}]^{\bullet+}$ (i.e., the cationic unit of **6**$^{\bullet}$). The predicted strong absorption at 537 nm compares to the experimental observation (588 nm) of **6**$^{\bullet}$, corresponding to the excitation from HOMO−1 to SOMO. An extremely weak absorption at 625 nm (due to the excitation from HOMO to SOMO) is also predicted, which is very similar to the experimental observation of 622 nm of **6**$^{\bullet}$.

The cyclic voltammetry (CV) experiment of **6**$^{\bullet}$ was conducted in THF with an external ferrocene/ferrocenium (Fc/Fc$^+$) standard. X-ray quality crystals of $[\mathbf{6}^{\bullet}]_2\cdot$**(1,2-difluorobenzene)**$_{4.5}$ were employed for this study. While radical **1**$^{\bullet}$ exhibits two electrochemically quasi-reversible redox peaks at $E_{1/2} = -0.78$ V ($\Delta E_p = 0.21$ V) and $E_{1/2} = -1.47$ V ($\Delta E_p = 0.25$ V), which correspond to $[L^0/L^{\bullet -}]$ and $[L^{\bullet -}/L^{2-}]$ ligand reduction events (L denotes the dithiolene ligand), respectively,[25] the cyclic voltammogram (Figure 2) of radical **6**$^{\bullet}$ exhibits a relatively complicated redox pattern in the potential range from +0.68 to −2.32 V (vs Fc$^{+/0}$). An irreversible oxidation process (at $E_{ox} = +0.01$ V) is assigned to the one-electron oxidation of **6**$^{\bullet}$ to corresponding neutral dithiolene-complexed (i.e., dithione, L^0) Mg^{2+} dication species, which is less stable than the lithium analogue[25] and may immediately participate in a subsequent chemical transformation. Consequently, no corresponding rereduction is observed when the voltage sweep is reversed (left to right in Figure 2), even at high scan rates (Figure S2). Indeed, according to the hard−soft acid−base concept, the “hard” Mg^{2+} cation is much less inclined to bind to “soft” sulfur-based ligands than to oxygen-based ligands.[26] For instance, Mg−S bonds are quite rare in nature, only having been observed in a chlorophyll chromophore in photosystem I.[27] Our efforts to obtain a dithione (L^0)-complexed Mg^{2+} species through a 1:2 reaction of **5** with $Ph_3C^+[B(C_6F_5)_4]^-$ were unsuccessful (and only resulted in the isolation of an imidazole-based dithione dimer).[25] The dithione (L^0)-complexed Mg^{2+} species, however, may exist as an elusive intermediate in the dithione−dimer formation. The reduction peaks between −0.63 and −1.09 V may be due to $[L^{\bullet -}/L^{2-}]$ ligand reduction events. The conversion of **6**$^{\bullet}$ into a radical derivative (containing the $L^{\bullet -}$ unit) during the CV experiments may be postulated, since there are two closely spaced, quasi-reversible redox couples [at $E_{1/2} = -0.77$ V ($\Delta E_p = 0.28$ V) and $E_{1/2} = -0.94$ V ($\Delta E_p = 0.31$ V)]. However, it has been reported that closely spaced peaks for redox couples may be observed during various scenarios such as axial ligand exchanges[28] and “radical−substrate” dimerization reactions.[29] The cause of reduction events occurring at more negative potentials (−1.1 to −2.3 V along the reduction sweep) remain unclear and investigating the mechanisms of reactions contributing to those small peaks is beyond the scope of this work.

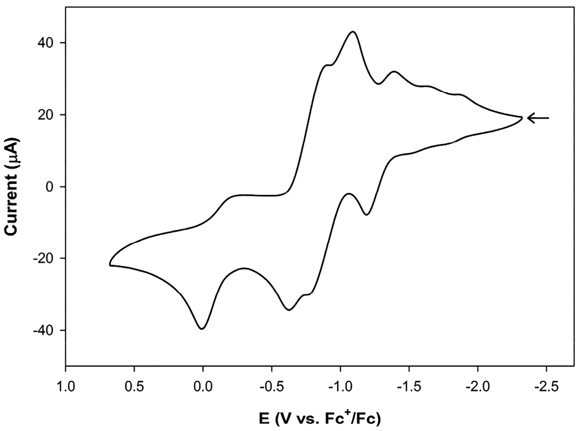

Figure 2. Cyclic voltammogram of **6**$^{\bullet}$ (3.8 mM) with Fc external standard (6.0 mM; $E_{1/2} = 0$ V) in THF (scan speed: 100 mV s^{-1}, 0.1 M $^n Bu_4NPF_6$ supporting electrolyte, glassy carbon working electrode, Pt-wire counter electrode, room temperature). The arrow indicates direction of the scan.

The room-temperature EPR spectrum of **6**$^{\bullet}$ (radical concentration: 3.1×10^{-4} M, estimated using SpinCount) is shown in Figure 3. The EPR spectrum displays an $S = 1/2$ quintet (Figure 3a), which was accurately simulated with hyperfine splitting on two equivalent nitrogen atoms (^{14}N, $I = 1$) using the Bruker SpinFit program and the model of the fast-motion limit with isotropic (or fully motional averaged) components of the g- and A-tensors. Spectral simulations give $g = 2.01168$ and hyperfine splitting constant of $a_N = 0.98$ G. The hyperfine splitting $a_N = 0.98$ G of **6**$^{\bullet}$ is nearly equal to that ($a_N = 1.00$ G) for the boron-based dithiolene radical (**3**$^{\bullet}$);[20] however, smaller than that of the lithium dithiolene radical (**1**$^{\bullet}$)[19] ($a_N = 1.39$ G) and naked dithiolene radical (**4**$^{\bullet}$)[21] ($a_N = 1.46$ G). The weak satellite feature of the EPR spectrum of **6**$^{\bullet}$ (Figure 3b) originates from an admixture of the ^{25}Mg isotope ($I = 5/2$) with a natural abundance of ca. 10%. This admixture yields six satellite lines with an intensity of each one ca. 2% relative to central line from the ^{24}Mg and ^{26}Mg nuclei having no nuclear spin ($I = 0$). These satellite lines overlap with the central peak and each other. An approximate estimate of the hyperfine splitting on ^{25}Mg can be also obtained with the SpinFit program. As seen in Figure 3b, the feature on the left side of the main peak can be reasonably well-simulated with an a_{Mg} value of 2.3 G. Notably, the satellite feature on the right side of the main peak is less pronounced (black line, in Figure 3b), indicative of motional effects, manifesting in incomplete averaging of the hyperfine splitting on the ^{25}Mg atoms, as well

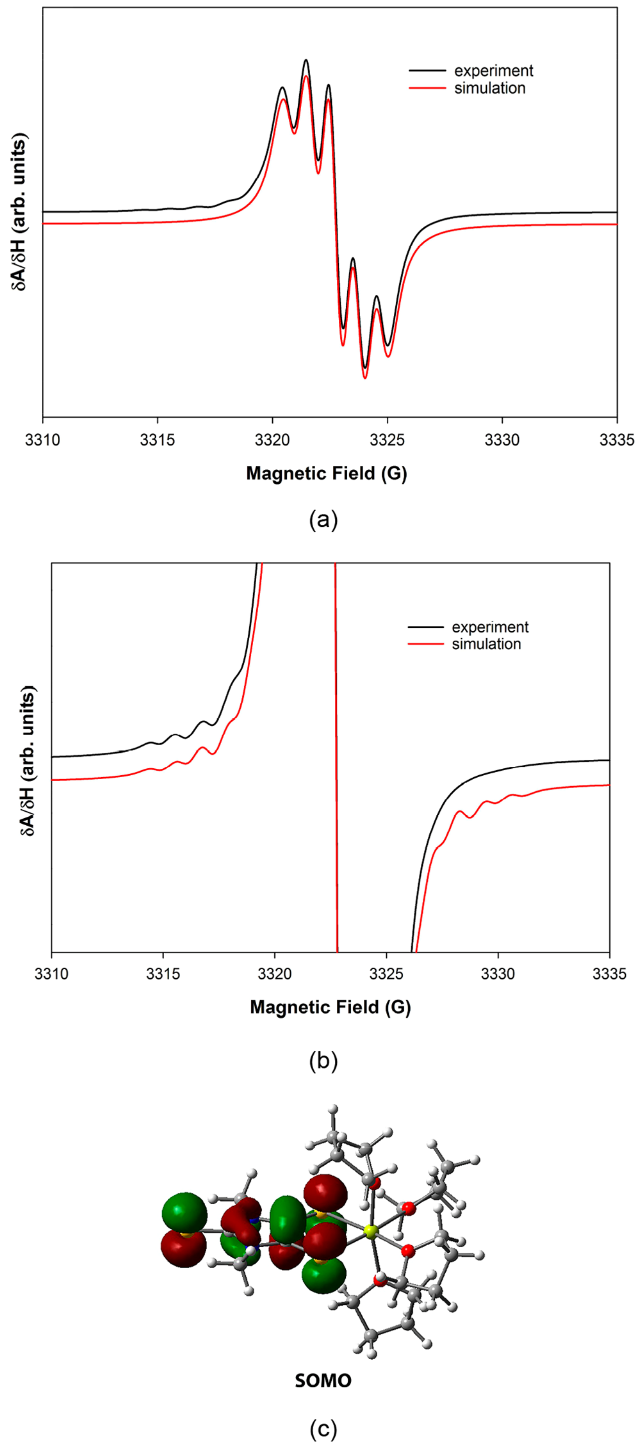

Figure 3. (a) Room-temperature X-band EPR spectrum of $\mathbf{6}^{\bullet}$ in toluene. The spectrum (black) was recorded at 9.356 GHz with a modulation amplitude of 0.1 G and a microwave power of 1.6 mW. Its simulation (red) used isotropic values of the *g*-factor and the hyperfine splitting ($g = 2.01168$, $a_N = 0.98$ G) and a line width of 0.86 G. (b) The satellite features of the EPR spectrum of $\mathbf{6}^{\bullet}$ due to the ^{25}Mg admixture (black). Simulation of these features (red) used an additional spectral component having the same spin-Hamiltonian and line width parameter, with an addition of a second ^{25}Mg nucleus ($I = 5/2$) and $a_{Mg} = 2.3$ G. The symmetric appearance of the simulation using the fast-motion limit model and lower intensity of the satellite lines in the experiment pointing to motional effects. (c) SOMO of $[\mathbf{6\text{-}Me}]^{\bullet+}$, the simplified model of the cationic unit of $\mathbf{6}^{\bullet}$.

as of the presence of some g-factor anisotropy (see the Supporting Information).[22]

Molecular orbital calculations[22] of simplified $[\mathbf{6\text{-}Me}]^{\bullet+}$ show that the SOMO is primarily dithiolene ligand-based, with C−C *π*-bonding and C−S *π*-antibonding character (Figure 3c). The spin density of $[\mathbf{6\text{-}Me}]^{\bullet+}$ resides predominantly at the C_2S_2 unit (0.70) and the terminal sulfur atom (0.28), which compare well with those for boron dithiolene radicals [C_2S_2 (0.71), $S_{terminal}$ (0.27) for $\mathbf{2}^{\bullet}$; C_2S_2 (0.77), $S_{terminal}$ (0.23) for $(\mathbf{3\text{-}Ph})^{\bullet}$].[20] In contrast to magnesium- and boron-based dithiolene radicals [i.e., $[\mathbf{6\text{-}Me}]^{\bullet+}$, $\mathbf{2}^{\bullet}$, and $\mathbf{3\text{-}Ph}^{\bullet}$], the lithium dithiolene radical $(\mathbf{1\text{-}Ph}^{\bullet})$[19] and anionic naked dithiolene radical $(\mathbf{4}^{\bullet-})$[21] display more spin density at the C_2S_2 units (0.88 for $\mathbf{1\text{-}Ph}^{\bullet}$ and 0.87 for $\mathbf{4}^{\bullet-}$) and concomitantly less spin density at the terminal sulfur atoms (0.18 for $\mathbf{1\text{-}Ph}^{\bullet}$ and 0.12 for $\mathbf{4}^{\bullet-}$; the $S_{terminal}$ atom in $\mathbf{4}^{\bullet-}$ denotes the sulfur atom next to the C2 carbon). In addition, the very low spin density (5.9×10^{-4}) residing at the magnesium atom in $[\mathbf{6\text{-}Me}]^{\bullet+}$ is consistent with the weak ^{25}Mg satellite lines observed in the EPR spectrum of $\mathbf{6}^{\bullet}$ (Figure 3).

X-ray structural analysis[22] of $\mathbf{6}^{\bullet}$ (Figure 4) reveals that the asymmetric unit contains two $\mathbf{6}^{\bullet}$ molecules which exist as separate magnesium-based dithiolene radical cation/$[B(C_6F_5)_4]^-$ anion pairs. For clarity, only the structural parameters of one $\mathbf{6}^{\bullet}$ molecule are shown in Figure 4. Being complexed by four THF molecules, the six-coordinate magnesium atom in $\mathbf{6}^{\bullet}$ adopts a distorted octahedral geometry. In contrast to the planar five-membered C_2S_2Mg ring in $\mathbf{5}$,[23] the C_2S_2Mg ring $\mathbf{6}^{\bullet}$ is slightly bent [bend angle (η) between the S_2Mg plane and the S_2C_2 plane = 177.2°, avg], which compares well to the theoretical value (174.7°) of $[\mathbf{6\text{-}Me}]^{\bullet+}$.[22] By comparison with the structural parameters of the C_2S_2Mg ring in $\mathbf{5}$ [$d_{C=C} = 1.360(6)$ Å; $d_{C-S} = 1.724(3)$ Å; $d_{Mg-S} = 2.5339(12)$ Å],[23] $\mathbf{6}^{\bullet}$ displays an elongated C=C bond (1.418 Å, avg), Mg−S bonds (2.599 Å, avg) and concomitantly shortened C−S bonds (1.683 Å, avg), which are consistent with the corresponding theoretical values of $[\mathbf{6\text{-}Me}]^{\bullet+}$ ($d_{C=C} =$

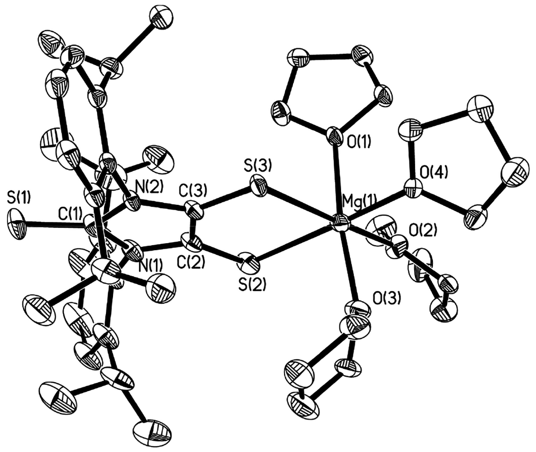

Figure 4. Molecular structures of the cationic unit of $\mathbf{6}^{\bullet}$. Thermal ellipsoids represent 30% probability; hydrogen atoms on carbon are omitted for clarity. Selected bond distances (Å) and angles (deg): C(1)−S(1) 1.654(4), C(2)−C(3) 1.420(5), C(2)−S(2) 1.678(4), C(3)−S(3) 1.687(4), Mg(1)−S(2) 2.6023(19), Mg(1)−S(3) 2.6135(16), Mg(1)−O(4) 2.091(4); S(2)−Mg(1)−S(3) 84.74(5), C(2)−S(2)−Mg(1) 99.40(14), C(3)−S(3)−Mg(1) 98.79(13), C(2)−C(3)−S(3) 128.6(3).

1.422 Å; d_{C-S} = 1.707 Å; d_{Mg-S} = 2.607 Å).[22] The Wiberg bond indices (WBIs) of the C═C bond (1.22) and C−S bond (1.29, avg) in the C_2S_2 unit of [**6-Me**]$^{\bullet+}$ indicate their modest double-bond character. The WBI (0.32) of Mg−S bonds in [**6-Me**]$^{\bullet+}$ is only marginally less than that (0.36) for **5**.[23] This fact supports the ionic bond essence of the Mg−S bond in these two compounds. In addition, the magnesium atom of [**6-Me**]$^{\bullet+}$ has a positive charge of +1.31, whereas each sulfur atom in the C_2S_2 unit bears a negative charge of −0.28.

CONCLUSIONS

The first cationic magnesium dithiolene radical (**6**$^{\bullet}$) was synthesized by 1:1 reaction of neutral magnesium dithiolate precursor (**5**) with $Ph_3C^+[B(C_6F_5)_4]^-$. The EPR study shows that the radical character of **6**$^{\bullet}$ is mainly ligand-based. The weak satellite lines should be due to the presence of ^{25}Mg hyperfine interaction.

EXPERIMENTAL SECTION

General. The syntheses of air-sensitive compounds were performed under purified argon using Schlenk techniques and an inert atmosphere drybox (M-Braun LabMaster SP). Chemicals were purchased from Aldrich and Strem and used as received. The solvents were dried and distilled under argon from Na/benzophenone prior to use. 1,2-difluorobenzene was distilled after a two-day reflux with CaH_2, and was then dried using 3A molecular sieves. EPR spectrum of **6**$^{\bullet}$ was measured using an EMXplus EPR spectrometer (Bruker, Billerica, MA). X-ray intensity data for **6**$^{\bullet}$, CCDC 2110267, was collected at temperatures of 135 K on a Bruker D8 Quest PHOTON 100 CMOS X-ray diffractometer system with Incoatec Microfocus Source (IμS) monochromated Mo Kα radiation (λ = 0.71073 Å, sealed tube) using phi- and omega-scan technique. The UV−visible absorption spectrum of **6**$^{\bullet}$ was recorded under argon gas protection in 1 cm cuvettes using a Varian Cary 5000 UV−vis−NIR spectrophotometer. Cyclic voltammetry (CV) was performed in a custom-made three-electrode cell, which, consisting of a glassy carbon working electrode (3 mm diameter, CHI104, CH Instruments), a nonaqueous Ag/Ag$^+$ (0.01 M $AgNO_3$/0.1 M $^nBu_4NPF_6$ in MeCN) reference electrode (CHI112, CH Instruments), and a platinum wire as the counter electrode, is connected to an electrochemical workstation/potentiostat (CHI920C, CH Instruments Inc., Austin, TX). Measurements were performed at ambient temperature using 3.8 mM analyte in THF under Ar containing 0.1 M $^nBu_4NPF_6$ as the supporting electrolyte. Analyte potentials were referenced against an external ferrocene (6.0 mM) standard ($E_{1/2}$ = 0.322 V in THF vs the Ag/Ag$^+$ reference electrode). Cyclic voltammograms were obtained between −2.0 and 1.0 V with a series of scan rates (i.e., 100, 200, 300, 400, and 500 mV s^{-1}) and a sampling interval of 0.001 V. Elemental analyses were performed by Complete Analytical Laboratories (Highland Park, NJ).

Compound 6$^{\bullet}$. First, 5 mL of toluene was added to a Schlenk tube containing **5** (0.300 g, 0.38 mmol) and $Ph_3C^+[B(C_6F_5)_4]^-$ (0.348 g, 0.38 mmol) at room temperature. After the mixture was stirred overnight, the volatile materials were removed in vacuo. The residue was rinsed with 20 mL of hexane and subsequently recrystallized in the 1,2-difluorobenzen/hexane mixed solvent at −40 °C, giving **6**$^{\bullet}$ as X-ray quality dark purple−blue crystals (0.398 g, 60.9% yield). Mp: gradually decomposed (>131.2 °C) and melt (>203.3 °C). UV−vis (λ/nm): 580, 622. Crystal data for [**6**$^{\bullet}$]$_2$·**(1,2-difluorobenzene)**$_{4.5}$: $C_{161}H_{150}B_2F_{49}Mg_2N_4O_8S_6$, fw = 3462.44, triclinic, $P\bar{1}$, a = 14.8827(16) Å, b = 23.769(3) Å, c = 23.805(3) Å, α = 76.499(3)°, β = 86.100(3)°, γ = 87.094(3)°, V = 8163.8(15) Å3, Z = 2, R_1 = 0.0777 for 20405 data ($I > 2\sigma(I)$), wR_2 = 0.2355 (all data). Anal. Calcd (found) (%) for **6**$^{\bullet}$ (1474.53): C 54.57 (54.10); H 4.51 (4.64); N 1.90 (1.79).

ASSOCIATED CONTENT

Supporting Information

The Supporting Information is available free of charge at https://pubs.acs.org/doi/10.1021/acs.organomet.1c00607.

Details of spectra, computations, and X-ray crystallography (PDF)

Cartesian coordinates for the calculated structure (XYZ)

Accession Codes

CCDC 2110267 contains the supplementary crystallographic data for this paper. These data can be obtained free of charge via www.ccdc.cam.ac.uk/data_request/cif, or by emailing data_request@ccdc.cam.ac.uk, or by contacting The Cambridge Crystallographic Data Centre, 12 Union Road, Cambridge CB2 1EZ, UK; fax: +44 1223 336033.

AUTHOR INFORMATION

Corresponding Author

Gregory H. Robinson − *Department of Chemistry and the Center for Computational Chemistry, The University of Georgia, Athens, Georgia 30602-2556, United States;* orcid.org/0000-0002-2260-3019; Email: robinson@uga.edu

Authors

Yuzhong Wang − *Department of Chemistry and the Center for Computational Chemistry, The University of Georgia, Athens, Georgia 30602-2556, United States;* orcid.org/0000-0003-3557-5085

Phuong M. Tran − *Department of Chemistry and the Center for Computational Chemistry, The University of Georgia, Athens, Georgia 30602-2556, United States;* orcid.org/0000-0003-2054-2862

Boris Dzikovski − *Bruker BioSpin Corporation, Billerica, Massachusetts 01821, United States;* orcid.org/0000-0002-5687-5207

Yaoming Xie − *Department of Chemistry and the Center for Computational Chemistry, The University of Georgia, Athens, Georgia 30602-2556, United States*

Pingrong Wei − *Department of Chemistry and the Center for Computational Chemistry, The University of Georgia, Athens, Georgia 30602-2556, United States;* orcid.org/0000-0001-7162-4142

April A. Rains − *Nano Electrochemistry Laboratory, School of Chemical, Materials and Biomedical Engineering, The University of Georgia, Athens, Georgia 30602-2556, United States;* orcid.org/0000-0002-9441-425X

Hamid Asadi − *Nano Electrochemistry Laboratory, School of Chemical, Materials and Biomedical Engineering, The University of Georgia, Athens, Georgia 30602-2556, United States;* orcid.org/0000-0002-5028-8351

Ramaraja P. Ramasamy − *Nano Electrochemistry Laboratory, School of Chemical, Materials and Biomedical Engineering, The University of Georgia, Athens, Georgia 30602-2556, United States*

Henry F. Schaefer, III − *Department of Chemistry and the Center for Computational Chemistry, The University of Georgia, Athens, Georgia 30602-2556, United States;* orcid.org/0000-0003-0252-2083

Complete contact information is available at: https://pubs.acs.org/10.1021/acs.organomet.1c00607

Notes

The authors declare no competing financial interest.

■ ACKNOWLEDGMENTS

We are grateful to the National Science Foundation for support: (CHE-1855641 to G.H.R. and Y.W.) (CHE-2134792 to H.F.S.). The EPR instrument was obtained with funds from the NSF Major Research Instrumentation (MRI) Grant No. 1827968.

■ REFERENCES

(1) Gray, H. B.; Billig, E. The Electronic Structures of Square Planar Metal Complexes. III. High-Spin Planar Cobalt(I) and Iron(I). *J. Am. Chem. Soc.* **1963**, *85*, 2019−2020.

(2) Stiefel, E. I.; Waters, J. H.; Billig, E.; Gray, H. B. The Myth of Nickel(III) and Nickel(IV) in Planar Complexes. *J. Am. Chem. Soc.* **1965**, *87*, 3016−3017.

(3) Sproules, S.; Wieghardt, K. Dithiolene Radicals: Sulfur K-Edge X-Ray Absorption Spectroscopy and Harry's Intuition. *Coord. Chem. Rev.* **2011**, *255*, 837−860.

(4) Kokatam, S.; Ray, K.; Pap, J.; Bill, E.; Geiger, W. E.; LeSuer, R. J.; Rieger, P. H.; Weyhermüller, T.; Neese, F.; Wieghardt, K. Molecular and Electronic Structure of Square-Planar Gold Complexes Containing Two 1,2-Di(4-tert-butylphenyl)ethylene-1,2-dithiolato Ligands: $[Au(^2L)_2]^{1+/0/1-/2-}$. *A Combined Experimental and Computational Study. Inorg. Chem.* **2007**, *46*, 1100−1111.

(5) Huyett, J. E.; Choudhury, S. B.; Eichhorn, D. M.; Bryngelson, P. A.; Maroney, M. J.; Hoffman, B. M. Pulsed ENDOR and ESEEM Study of $[Bis(maleonitriledithiolato)nickel]^-$: An Investigation into the Ligand Electronic Structure. *Inorg. Chem.* **1998**, *37*, 1361−1367.

(6) Milsmann, C.; Patra, G. K.; Bill, E.; Weyhermüller, T.; DeBeer George, S.; Wieghardt, K. Octahedral Monodithiolene Complexes of Iron: Characterization of S,S'-Coordinated Dithiolate(1-) π Radical Monoanions: A Spectroscopic and Density Functional Theoretical Investigation. *Inorg. Chem.* **2009**, *48*, 7430−7445.

(7) Milsmann, C.; Bothe, E.; Bill, E.; Weyhermüller, T.; Wieghardt, K. Octahedral Monodithiolene Complexes of Cobalt(III) and Chromium(III). Spectroscopic and Density Functional Theoretical Characterization of S,S'-Coordinated Benzene-1,2-dithiolate(1-) π Radicals. *Inorg. Chem.* **2009**, *48*, 6211−6221.

(8) Szilagyi, R. K.; Lim, B. S.; Glaser, T.; Holm, R. H.; Hedman, B.; Hodgson, K. O.; Solomon, E. I. Description of the Ground State Wave Functions of Ni Dithiolenes Using Sulfur K-Edge X-Ray Absorption Spectroscopy. *J. Am. Chem. Soc.* **2003**, *125*, 9158−9169.

(9) Sarangi, R.; DeBeer George, S.; Rudd, D. J.; Szilagyi, R. K.; Ribas, X.; Rovira, C.; Almeida, M.; Hodgson, K. O.; Hedman, B.; Solomon, E. I. Sulfur K-Edge X-Ray Absorption Spectroscopy as a Probe of Ligand-Metal Bond Covalency: Metal vs Ligand Oxidation in Copper and Nickel Dithiolene Complexes. *J. Am. Chem. Soc.* **2007**, *129*, 2316−2326.

(10) Kapre, R. R.; Bothe, E.; Weyhermüller, T.; DeBeer George, S.; Wieghardt, K. Electronic Structure of Neutral and Monoanionic Tris(benzene-1,2-dithiolato) Metal Complexes of Molybdenum and Tungsten. *Inorg. Chem.* **2007**, *46*, 5642−5650.

(11) Ray, K.; DeBeer George, S.; Solomon, E. I.; Wieghardt, K.; Neese, F. Description of the Ground-State Covalencies of the Bis(dithiolato) Transition-Metal Complexes from X-Ray Absorption Spectroscopy and Time-Dependent Density-Functional Calculations. *Chem. - Eur. J.* **2007**, *13*, 2783−2797.

(12) Tenn, N.; Bellec, N.; Jeannin, O.; Piekara-Sady, L.; Auban-Senzier, P.; Iniguez, J.; Canadell, E.; Lorcy, D. A Single-Component Molecular Metal Based on a Thiazole Dithiolate Gold Complex. *J. Am. Chem. Soc.* **2009**, *131*, 16961−16967.

(13) Filatre-Furcate, A.; Bellec, N.; Jeannin, O.; Auban-Senzier, P.; Fourmigue, M.; Vacher, A.; Lorcy, D. Radical or Not Radical: Compared Structures of Metal (M = Ni, Au) Bis-Dithiolene Complexes with a Thiazole Backbone. *Inorg. Chem.* **2014**, *53*, 8681−8690.

(14) Attar, S.; Espa, D.; Artizzu, F.; Mercuri, M. L.; Serpe, A.; Sessini, E.; Concas, G.; Congiu, F.; Marchio, L.; Deplano, P. A Platinum-Dithiolene Monoanionic Salt Exhibiting Multiproperties, Including Room-Temperature Proton-Dependent Solution Luminescence. *Inorg. Chem.* **2016**, *55*, 5118−5126.

(15) Russell, G. A.; Zaleta, M. Applications of ESR Spectroscopy to Problems of Structure and Conformation. 34. Dithiaethylene Radical Cations and Anions. *J. Am. Chem. Soc.* **1982**, *104*, 2318.

(16) Russell, G. A.; Law, W. C.; Zaleta, M. Aliphatic Semidiones.44. Spin Probes Derived from Dithiols. *J. Am. Chem. Soc.* **1985**, *107*, 4175−4182.

(17) Buddensiek, D.; Köpke, B.; Voss, J. Thioketyls. 9. ESR Studies and Semi-Empirical MO Calculations on Mono- and Dithiosemidione Radical Anions. *Chem. Ber.* **1987**, *120*, 575−81.

(18) Roth, B.; Bock, H.; Gotthardt, H. Radical ions. 66. Thioparabanic Acid Derivatives: Ionization to the Radical Cation and Reduction to the Radical Anion. *Phosphorus, Sulfur Relat. Elem.* **1985**, *22*, 109−119.

(19) Wang, Y.; Hickox, H. P.; Xie, Y.; Wei, P.; Blair, S. A.; Johnson, M. K.; Schaefer, H. F., III; Robinson, G. H. A Stable Anionic Dithiolene Radical. *J. Am. Chem. Soc.* **2017**, *139*, 6859−6862.

(20) Wang, Y.; Xie, Y.; Wei, P.; Blair, S. A.; Cui, D.; Johnson, M. K.; Schaefer, H. F., III; Robinson, G. H. Stable Boron Dithiolene Radicals. *Angew. Chem., Int. Ed.* **2018**, *57*, 7865−7868.

(21) Wang, Y.; Xie, Y.; Wei, P.; Blair, S. A.; Cui, D.; Johnson, M. K.; Schaefer, H. F., III; Robinson, G. H. A Stable Naked Dithiolene Radical Anion and Synergic THF Ring-Opening. *J. Am. Chem. Soc.* **2020**, *142*, 17301−17305.

(22) See the Supporting Information for spectral, computational, and crystallographic details.

(23) Wang, Y.; Maxi, N. A.; Xie, Y.; Wei, P.; Schaefer, H. F., III; Robinson, G. H. Lewis Base-Complexed Magnesium Dithiolenes. *Chem. Commun.* **2019**, *55*, 8087−8089.

(24) Peach, M. J. G.; Benfield, P.; Helgaker, T.; Tozer, D. J. Excitation Energies in Density Functional Theory: An Evaluation and a Diagnostic Test. *J. Chem. Phys.* **2008**, *128*, No. 044118.

(25) Wang, Y.; Xie, Y.; Wei, P.; Schaefer, H. F., III; Robinson, G. H. Redox Chemistry of an Anionic Dithiolene Radical. *Dalton Trans.* **2019**, *48*, 3543−3546.

(26) Rappoport, Z., Marek, I., Eds. *The Chemistry of Organomagnesium Compounds*; John Wiley & Sons, Ltd.: Chichester, U.K., 2008.

(27) Jordan, P.; Fromme, P.; Witt, H. T.; Klukas, O.; Saenger, W.; Krauss, N. Three-Dimensional Structure of Cyanobacterial Photosystem I at 2.5 Angstrom Resolution. *Nature* **2001**, *411*, 909−917.

(28) Lawrence, M. A. W.; Celestine, M. J.; Artis, E. T.; Joseph, L. S.; Esquivel, D. L.; Ledbetter, A. J.; Cropek, D. M.; Jarrett, W. L.; Bayse, C. A.; Brewer, M. I.; Holder, A. A. Computational, Electrochemical, and Spectroscopic Studies of Two Mmononuclear Cobaloximes: the Influence of an Axial Pyridine and Solvent on the Redox Behaviour and Evidence for Pyridine Coordination to Cobalt(I) and Cobalt(II) Metal Centres. *Dalton Trans.* **2016**, *45*, 10326−10342.

(29) Nafady, A.; Alsalme, A. M.; Al-Farhan, K. A.; El Khatib, R. M.; Bhargava, S. Probing Solvation and Ion-Pairing Effects on the Redox Behavior of Cyclopentadienyl Cobalt Dicarbonyl, $CpCo(CO)_2$, in the presence of $[B(C_6F_5)_4]^-$ Anion. *Int. J. Electrochem. Sci.* **2014**, *9*, 8131−8144.